J Neurophysiol 91: 1314–1326, 2004.
First published October 8, 2003; 10.1152/jn.00637.2003.

Optic Flow Signals in Extrastriate Area MST: Comparison of Perceptual and Neuronal Sensitivity

Hilary W. Heuer[1] and Kenneth H. Britten[1,2]
[1]*Center for Neuroscience and* [2]*Section of Neurobiology, Physiology and Behavior, University of California, Davis, California 95616*

Submitted 3 July 2003; accepted in final form 3 October 2003

Heuer, Hilary W. and Kenneth H. Britten. Optic flow signals in extrastriate area MST: comparison of perceptual and neuronal sensitivity. *J Neurophysiol* 91: 1314–1326, 2004. First published October 8, 2003; 10.1152/jn.00637.2003. The medial superior temporal area of extrastriate cortex (MST) contains signals selective for nonuniform patterns of motion often termed "optic flow." The presence of such tuning, however, does not necessarily imply involvement in perception. To quantify the relationship between these selective neuronal signals and the perception of optic flow, we designed a discrimination task that allowed us to simultaneously record neuronal and behavioral sensitivities to near-threshold optic flow stimuli tailored to MST cells' preferences. In this two-alternative forced-choice task, we controlled the salience of globally opposite patterns (e.g., expansion and contraction) by varying the coherence of the motion. Using these stimuli, we could both relate the sensitivity of neuronal signals in MST to the animal's behavioral sensitivity and also measure trial-by-trial correlation between neuronal signals and behavioral choices. Neurons in MST showed a wide range of sensitivities to these complex motion stimuli. Many neurons had sensitivities equal or superior to the monkey's threshold. On the other hand, trial-by-trial correlation between neuronal discharge and choice ("choice probability") was weak or nonexistent in our data. Together, these results lead us to conclude that MST contains sufficient information for threshold judgments of optic flow; however, the role of MST activity in optic flow discriminations may be less direct than in other visual motion tasks previously described by other laboratories.

INTRODUCTION

Visual motion is created by objects moving in the environment or by self-motion through the world. Whatever the source, visual motion is generally believed to be processed in a functionally specialized pathway in visual cortex, the "dorsal stream." Early stages of this pathway, such as the middle temporal area (MT), are selective for uniform linear motion patterns (Orban 1997). However, much of the motion experienced by organisms under normal conditions consists of more complex, spatially nonuniform motion, or "optic flow" (Gibson 1950).

Response selectivities for such complex patterns of motion first become evident in the medial superior temporal area (MST), a relatively high-level area in this cortical pathway. Neurons in MST show selective tuning for patterns such as expansion, contraction, rotation, or combinations thereof (Duffy and Wurtz 1991a,b; Saito et al. 1986; Tanaka and Saito 1989; Tanaka et al. 1986). Thus it is natural to consider MST as a likely substrate for the perception of optic flow, including heading stimuli—optic flow patterns that simulate trajectories experienced through self-navigation in the world (Bradley et al. 1996; Duffy and Wurtz 1995; Froehler 2002; Page and Duffy 1999; Paolini et al. 2000). Additionally, perturbing activity in MST with electrical microstimulation during the performance of a complex heading perception task (Britten and Van Wezel 2002; Britten and Van Wezel 1998) or a linear direction discrimination task (Celebrini and Newsome 1995) influences perceptual judgments. Together, these studies suggest that area MST is indeed involved in optic flow perception but do not elucidate the relationship between the activity of individual neurons and behavioral ability. To examine this issue, we recorded the responses of single neurons in MST of awake behaving monkeys while the monkeys performed a psychophysical discrimination of specified locally and globally opposite optic flow patterns that were optimized for each neuron's stimulus preferences. We were thus able to simultaneously measure both behavioral and neuronal sensitivity to optic flow patterns under conditions where the neuronal signal was most likely to be relevant to the perceptual judgment. These measurements allowed us to address directly whether the sensitivity of MST neurons for optic flow patterns was sufficient to support perceptual judgments of complex motion. In addition, this approach allowed us to investigate the possibility of correlation between neuronal response and behavioral choice on a trial-by-trial basis. Preliminary results of this study have previously appeared as abstracts (Heuer and Britten 1999, 2000).

METHODS

Preparation

Two adult rhesus macaques (*Macaca mulatta*) were used in this study: one male and one female. Prior to recording, each monkey was implanted with a stainless steel head restraint post and a scleral search coil (Judge et al. 1980) to monitor eye position. After each monkey completed training on the psychophysical task, a recording chamber was surgically placed over occipital cortex. For recording sessions, a stainless steel transdural guide tube was inserted at known locations within a plastic coordinate grid (Crist et al. 1988). A tungsten microelectrode (FHC) was introduced through the guide tube and advanced using a stepping motor microdrive (National Aperture).

We used both physiological and anatomical landmarks to localize area MST on the anterior bank of the superior temporal sulcus (STS). These landmarks included recording depth from the dural surface, gray matter/white matter transitions, and receptive field (RF) size (Tanaka et al. 1986; Van Essen et al. 1981). On a few penetrations near the floor of the STS, the transition from area MT to MST was

Address for reprint requests and other correspondence: K. H. Britten, Center for Neuroscience, Univ. of California, 1544 Newton Ct., Davis, CA 95616 (E-mail: khbritten@ucdavis.edu).

The costs of publication of this article were defrayed in part by the payment of page charges. The article must therefore be hereby marked "*advertisement*" in accordance with 18 U.S.C. Section 1734 solely to indicate this fact.

ambiguous; for these penetrations, only cells with large RFs that clearly included the fovea or were entirely ipsilateral were included. Generally, these cells were found after an abrupt discontinuity in retinotopy; they account for a small proportion (approximately 5%) of our sample and did not noticeably differ in their results.

After we located MST, we isolated and recorded single-unit activity using standard extracellular techniques. Electrode signals were amplified and filtered: single units were isolated with a window-discriminator (Bak Electronics) and their action potentials converted to TTL pulses. We used the public domain software package REX (Hays et al. 1982) to record the time of stimulus events and action potentials with 1-ms resolution.

Stimuli

All stimuli were presented on a CRT monitor (Mitsubishi Diamond Pro 21TX) that subtended 80° horizontally by 60° vertically at a viewing distance of 28 cm from the monkey. Pixel resolution was 1280 × 1024, with a vertical refresh rate of 72 Hz, corresponding to a frame interval of 13.9 ms. The stimuli were generated using custom software on a Pentium computer with a video card (ATI Mach 64) running in 8-bit grayscale mode. For the primary experiments described here, the background luminance was 10 cd/M^2, and the foreground was 60 cd/M^2, resulting in a Michelson contrast of 70%. The monitor was regularly calibrated to establish a linear luminance profile. Dots were presented within circular apertures, at a constant average density of 0.12 dots/deg^2. Dots were randomly generated, and each stimulus was generated with a new seed.

The random dot patterns employed consisted of a subset of optic flow patterns termed "spiral space" by Graziano et al. (1994). Spiral space can be formalized as a pair of orthogonal axes, with radial motion on one axis and rotary motion on the other (Fig. 1*A*). Intermediate directions are spirals—combinations of rotation and radial motion, such as an expanding counter-clockwise pattern. To vary the strength of these stimuli, we used a technique previously applied to linear direction stimuli (Britten et al. 1992; Celebrini and Newsome 1994). This technique varies the stimulus strength by changing the percentage of dots that are replotted in a manner consistent with the specified direction pattern. We varied this percentage, and thus the motion strength, by setting the probability that each dot would be repositioned in this manner. We refer to the proportion of dots that carry the specified motion pattern as the percent coherence. A stimulus that is fully coherent has all the dots replotted with the appropriate spatial and temporal offsets to produce an apparently smooth motion pattern. The opposite extreme, the 0% coherence stimulus, contains only dots that are randomly repositioned, forming "white" motion noise (see Fig. 1*B* for schematic examples). The speed of the stimulus dots increased linearly from the center of the stimulus to the edge.

RF mapping and stimulus optimization

Once a neuron was isolated, we determined the RF location and size using handheld moving bar stimuli or computer-generated moving dot patches. Many neurons were only weakly responsive to the handheld moving bar stimuli; for these, we used dot patterns of varying size to estimate the receptive field boundaries. Some neurons showed sensitivity to eye position within the orbit, as previously reported (Squatrito and Maioli 1996, 1997); for these cells, we attempted to maximize response due to both eye position and stimulus extent. We positioned the stimuli within the RF for maximal response. When a cell's RF exhibited a "hot spot" of greater excitability, we placed stimuli over the hot spot and may not have filled the entire RF. For the remaining cells, we placed the stimuli to maximize areal extent within the RF without extending past the RF edges. Once we determined stimulus size and location, we undertook parametric optimization of the stimulus. We initially approximated both preferred spiral space direction and preferred speed qualitatively.

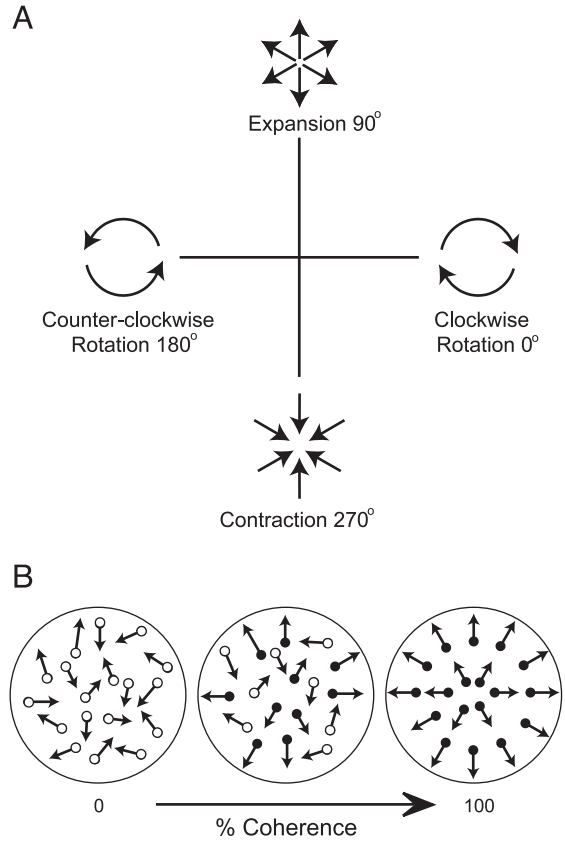

FIG. 1. *A*: stimulus space (Graziano et al. 1994). *B*: schematic demonstration of altering the motion strength for an expansion stimulus. Coherence increases from *left* to *right*.

Following the initial estimates of location and speed, we obtained quantitative direction tuning data. We presented eight directions of spiral space motion, equally spaced at 45° intervals, and eight directions of linear motion. The direction tuning stimuli were presented as highly coherent (75%) dot patterns; 100% coherent patterns were not used to minimize dot density artifacts. Generally, trials consisted of three stimuli of 500-ms duration, with 500-ms intervals between stimuli. For some cells, trials consisting of two stimuli of 1-s duration were used; there was no significant difference between the two measurements for cells where data were collected in both ways. The different directions of linear and spiral space were presented in a random sequence until responses were collected for a minimum of five repetitions of each motion pattern. We then fit these data with Gaussian functions to obtain a measure of the neuron's preferred direction. Such fits have previously been shown to describe accurately the direction tuning of MST cells to this family of stimuli (Graziano et al. 1994).

Psychophysical discrimination task

The primary data described here were collected while the monkeys performed a psychophysical discrimination between opposite spiral space directions. For each session, the directions for the behavioral discrimination were set to be the neuron's preferred stimulus and its opposite (or "null"). These directions were determined from the Gaussian fit to the tuning data (see Fig. 4*A* for example). The direction of the stimulus was randomly varied from trial to trial between the opposed alternatives; the monkey's task was to accurately identify which pattern was presented. The strength of the motion signal was

also varied systematically using log-spaced coherence levels chosen to span both neuronal and behavioral thresholds.

A schematic representation of task timing and geometry is shown in Fig. 2. Each trial began with the appearance of the fixation point. Once the monkey fixated, the stimulus appeared for 1 s. The monkey was required to maintain fixation throughout the stimulus period. When the stimulus disappeared, the monkey continued to fixate for 250 ms, followed by the onset of the two targets. This intervening fixation period allowed us to segregate temporally the neuron's response to the stimulus from any response evoked by the target onset. Targets were smaller random dot patches (6° diam); each target contained one of the two alternative motion patterns at high coherence (80%). This design allowed target geometry to be flexible; the monkey could learn each new geometrical configuration by using the information provided by the matching targets. Furthermore, even if the monkeys were performing a match on every trial, it would have negligible influence on our results, since performance would always be limited by the lower coherence of the first stimulus. The targets were usually positioned to require saccades of approximately equal magnitude to either target and were placed in different quadrants of the visual field, and their positions were held constant through each block of trials. Fixation was enforced for an additional 150 ms to allow visual inspection of the targets. The fixation point was extinguished, signaling the monkey to saccade to the target whose direction matched that of the initial stimulus. The monkey received a juice reward for correct discriminations; incorrect choices were followed by a brief "time-out" period (usually 1,500 ms) and a short tone. The monkey was randomly rewarded with a probability of 0.5 on trials where there was no net motion pattern (0% coherence) because there was no objectively correct answer for these stimuli.

Curve-fitting procedures

All descriptive fits of our data were performed using a maximum-likelihood, iterative fitter (Chandler 1965), and nested likelihood ratio analysis was used to determine the comparative quality of the resulting fits. We used this approach when the equations fit were variants of the same function with differing numbers of free parameters (Hoel et al. 1971). We transformed the likelihoods obtained from each fit by

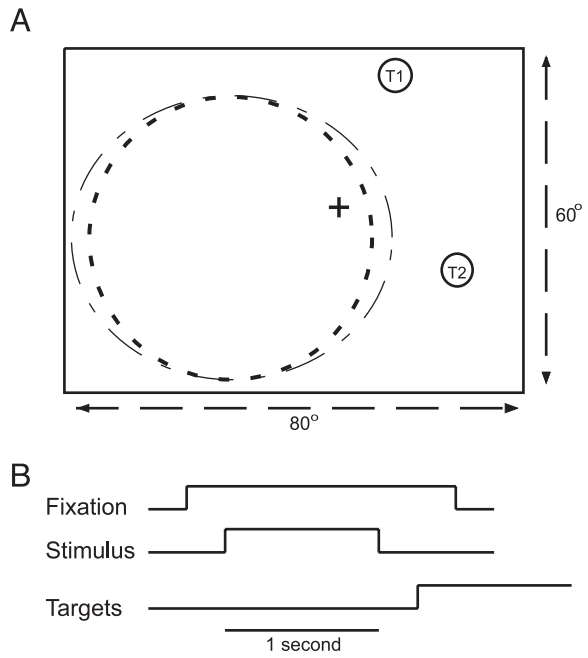

FIG. 2. Schematic indication of trial geometry. *A*: box indicates screen size; FP, fixation point; T1 and T2, example target locations; dashed line, receptive field; dotted line, stimulus aperture. *B*: relative timing of trial events.

$$\lambda = -2\ln(L(\text{data reduced function})/L(\text{data expanded function}))$$

λ is distributed approximately as χ^2, where the degrees of freedom are the additional number of free parameters in the expanded function. If λ exceeded the critical value for the degrees of freedom, we concluded that the expanded version provided a significantly better account of the data.

Analysis of psychophysical data

Behavioral data were analyzed as a function of motion coherence (%). For each level of motion strength, we calculated the proportion of correct choices, collapsed across the two directions of motion to form a psychometric function. We fit these data with a modified Quick (1974) function

$$p = 1 - 0.5\exp[(c/\alpha)]^{\beta}$$

where c is motion strength (percent coherence) and α indicates the monkey's threshold, or the motion strength level at which the monkey reliably gets 82.5% correct. β indicates the slope of the function, or how sharply the monkey's performance improves as a function of coherence. This analysis method has been described previously in greater detail in the context of a linear direction discrimination task (Britten et al. 1992; Celebrini and Newsome 1994).

Analysis of physiological data

The primary experiment compared neuronal sensitivity to perceptual sensitivity for spiral space motion patterns. To provide this direct comparison, we analyzed our physiological data to produce "neurometric functions" analogous to the psychometric functions used to describe the behavioral data. This method has been used in a variety of contexts (Bradley et al. 1987; Britten et al. 1992; Celebrini and Newsome 1994; DeAngelis and Uka 2003). Effectively, this method allows a calculation of the discriminability of direction based solely on neuronal firing rate.

To generate the neurometric function for each cell, we calculated the neuron's responses to individual stimulus presentations. Unless otherwise specified, all neuronal responses were analyzed as the total spike count for the duration of the visual stimulus, shifted 50 ms to account for neuronal latency. We required $\geq$10 stimulus repetitions for each condition (range, 10–45; mean, 17). For each coherence (motion strength), we compiled two distributions of these responses: one for stimuli in the preferred spiral space direction and a separate distribution for anti-preferred (null) stimuli. To compare these distributions, we assumed the existence of a neuron with equal and opposite tuning in spiral space [the "anti-neuron" (Britten et al. 1992)]. The response distributions were then assigned to neuron and anti-neuron according to preferred direction, allowing us to evaluate the discrimination performance for each stimulus level using receiver operator characteristic (ROC) analysis (Green and Swets 1966). We were then able to fit these ROC values with the same equation as our psychophysical data (*Eq. 2*) to obtain a neurometric function that was directly comparable to the monkey's simultaneously measured psychometric function.

One might wonder about the choice of an opponent formulation for the neurometric function, given that there is little evidence for direct opponency between neurons tuned for opposite directions of optic flow. We believe that this choice is sensible, because the opponency in the model has more to do with the readout of the representation. In our task, two opposite directions are being compared. Thus a sensible decision rule would be to compare the weight of evidence in favor of each alternative to form a decision (Gold and Shadlen 2002). While the representation of complex motion is distinctly biased in favor of expansion (Graziano et al. 1994), this does not effect the outcome in any fundamental way. Pools representing each alternative direction may differ in size, which would affect the performance of a popula-

tion-based analysis. However, for the opponent analysis of single neuron signals, the presence of all directions in the population representation is sufficient.

We measured the neurometric functions of 112 neurons in two monkeys. Seven of these cells were discarded from analysis due to poor behavioral performance during the psychophysical task; these were cases where the monkey's psychometric function was nonmonotonic or did not reach ≥95% correct at the highest coherence tested. Due to the poor behavioral performance, the comparison between neuronal and psychophysical sensitivity was invalid for these seven cases.

Of the remaining 105 cases, an additional 15 cells were excluded because their neurometric functions were not significantly better fit by the Quick function than by a constant value (nested log-likelihood test; $P < 0.05$, df = 3). These cells were ones that responded significantly above baseline to spiral space stimuli during the direction tuning series but were only weakly directional even at the high coherence used for the tuning measurements. This weak directionality did not produce a significant neurometric function across motion strengths.

Calculation of choice probability

To examine the relationship between neuronal activity and behavioral choice on a trial-by-trial basis, we computed a "choice probability" for each cell.

For each cell, we created two distributions of neuronal response sorted by the monkey's choice. Only conditions where the monkey made at least three choices in each direction were included. To avoid stimulus-dependent effects due to different firing rate means for each condition, we Z-transformed all spike counts before combining the data across conditions. Before combining the data in this way, we verified that there was no systematic variation in choice probability as a function of motion strength (data not shown). This allowed us to calculate a single pair of distributions of Z-transformed firing rates for preferred and null choices for each cell. These distributions were used to calculate the choice probability by ROC analysis.

To test the significance of observed choice probability values, we used a bootstrap method. For the bootstrap test, we randomly reassigned each trial's Z-score to the preferred or null distribution. This dissociated the response from the behavioral choice without distorting the relative proportion of preferred and null choices. We then calculated the choice probability for the permuted distributions; we repeated this manipulation for 2,500 iterations, allowing us to estimate the probability the observed value would occur by chance.

RESULTS

Behavioral results

Perceptually, the monkeys were sensitive to the spiral space stimuli used in these experiments, although thresholds differed significantly between the two monkeys. Monkey H had thresholds that were significantly higher than those of monkey F; average thresholds for the two monkeys were 14.5 and 5.9% coherence, respectively. Thresholds were measured for two human observers (1 naïve), who were instructed to use the full global motion pattern to perform the task, as opposed to local motion features. For central stimuli, thresholds for the two observers were 4.5 and 6.7%, respectively. Thus one of our monkeys performed similarly as did human observers on our task, while the other did not.

The threshold difference between the two monkeys could not be accounted for by differing stimulus parameter distributions for each monkey. Parameters for each experimental session were matched to the stimulus preferences of the neuron under study and therefore could have differed between the two monkeys. The primary stimulus parameters that varied across experiments were the preferred direction, speed, size, and eccentricity of the stimuli. In our analysis, we considered whether these parameters varied between the experiments conducted on each monkey and whether they influenced threshold measurements. While some stimulus parameters were related to psychophysically measured thresholds, none of these relationships was able to explain the observed threshold differences.

Neither stimulus direction nor speed was capable of explaining the monkey threshold differences. There was no correlation between preferred direction (as determined for the cell under study) and the monkey's threshold for that session (linear − circular correlation; Mardia and Jupp 2000; $P > 0.05$). In contrast, faster stimulus speeds systematically were correlated with higher behavioral thresholds ($r = 0.332$; $P = 0.0015$), although this correlation was not significant for each monkey's data considered individually ($r = 0.191$ and 0.236; $P > 0.1$). This correlation between speed and psychophysical performance did not explain the differences between the two monkeys' thresholds because speeds were similar for both monkeys ($t = -1.451$, $P > 0.1$).

Stimulus size and eccentricity showed a more complicated relationship with threshold; this relationship differed between the monkeys (Fig. 3). While the average stimulus size (diameter) differed between the two monkeys ($t = -2.104$, $P = 0.038$), this parameter only affected the behavioral thresholds of monkey F. Monkey F showed a significant correlation between stimulus diameter and threshold ($r = -0.327$; $P = 0.0149$), but monkey H did not ($r = 0.320$; $P = 0.0605$). On the other hand, eccentricity was sampled similarly between the two monkeys, and again only one monkey (H) showed a significant relationship between eccentricity and threshold ($r = 0.367$, $P = 0.0301$). Across the data from both monkeys, stimulus eccentricity had a significant effect ($r = 0.309$, $P = 0.003$) on thresholds, but the stimulus size did not. Thus individual stimulus parameters did not systematically appear to affect the thresholds in a way that would explain the observed substantial threshold difference. Individual thresholds are known to vary widely on many tasks, of course, both for monkeys and humans. As we will describe later, we found that neuronal thresholds did not differ between the animals as much as did their perceptual thresholds.

We were concerned that monkey H might have employed

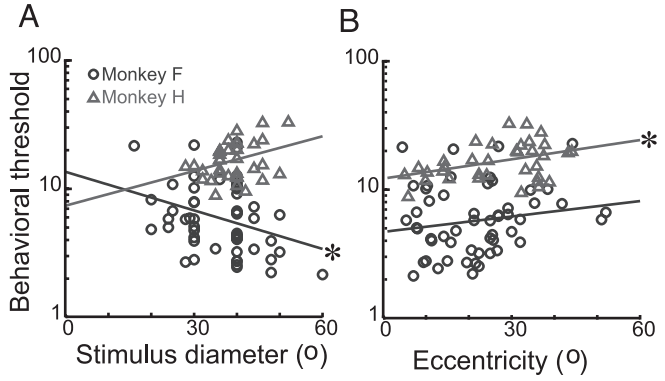

FIG. 3. Behavioral thresholds (percent coherence) as a function of stimulus parameters; solid lines indicate linear regressions. *Significant correlations.

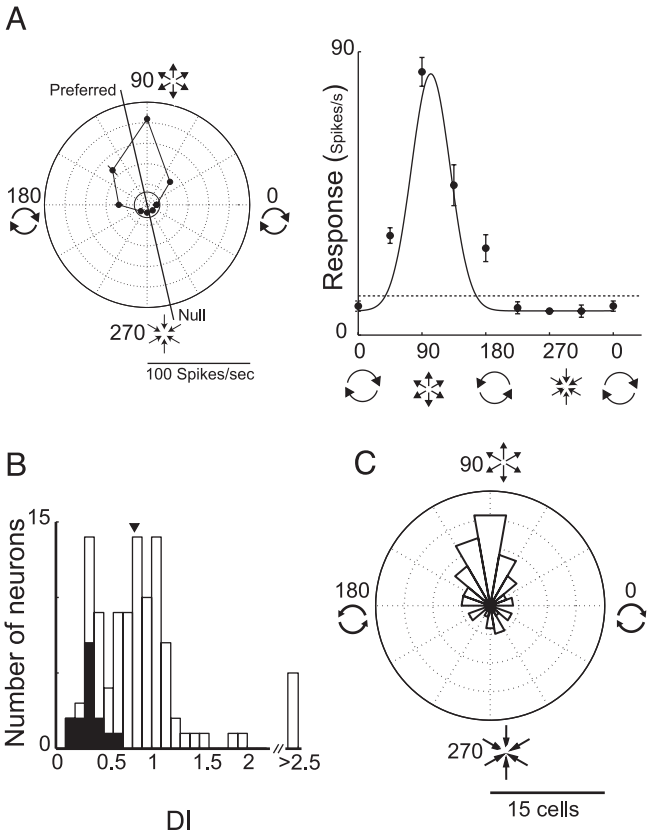

FIG. 4. Population description. *A*: single example cell, with a preferred direction of 106° in spiral space. Directionality index (DI) for this cell was 1.07. *B*: distribution of direction indices [1 − (null-ma/pref-ma)] estimated from Gaussian fits; ▽, population median (0.82). Solid bars, cells excluded from further analysis; median DI for included cells was 0.91. *C*: rose diagram of preferred directions for cells that passed inclusion criteria ($n = 90$). Each bin represents 15° in spiral space; size of wedge indicates number of cells whose preferred direction falls within that 15°. No correlation was found between DI and the preferred direction.

more local cues than did monkey F, which might have explained his higher thresholds. To test for this, we performed a separate series of psychophysical experiments, using foveally centered displays. We measured thresholds for a 10° diam pattern and a 40° pattern, which differed by over a factor of 5 (19.6 and 3.4% coherence, respectively). The large decrease in threshold by the addition of eccentric signal suggests that this monkey was not strictly attending to local cues, but instead, was integrating across larger areas when these were available.

Neuronal response properties

The neurons in our sample were heterogeneous, yet typical of MST in their response properties for spiral space stimuli. In Fig. 4*A*, we show an example cell's responses to eight directions of spiral space along with the axis used for the behavioral discrimination. The Gaussian fit to these responses was used to calculate a standard directionality index (DI) for each cell; the distribution of these DIs is shown in Fig. 4*B*. The filled bars depict the 15/105 cases that were excluded from further analyses due to flat neurometric functions. As seen in Fig. 4*C*, the distribution of preferred spiral space directions peaked near 90° (expansion). This anisotropy is consistent with previous reports (Geesaman and Andersen 1996; Graziano et al. 1994; Saito et al. 1986; Tanaka and Saito 1989; Tanaka et al. 1989).

Comparison of perceptual and neuronal sensitivity

Neuronal responses for preferred and null direction spiral space patterns diverged as a function of motion strength (Fig. 5), suggesting that individual neurons could be quite sensitive to these motion patterns. However, our primary question was whether the sensitivity of neurons in MST is sufficient to underlie perceptual sensitivity. To address this, we used ROC analysis to calculate a "neurometric" function for each cell as described in M[SCAP]ETHODS. This allowed a direct comparison of behavioral and neuronal sensitivity using the same metric for both.

The comparison of neuronal and perceptual sensitivity yielded a wide range of results (Fig. 6). Each column shows data from one monkey. In some cases, the neuron was more sensitive than the monkey was behaviorally (Fig. 6, *A* and *B*). In other experiments (Fig. 6, *C* and *D*), the neurometric and psychometric functions were quite similar and did not differ significantly. We also observed many cases where the neuron was significantly less sensitive than the monkey (Fig. 6, *E* and

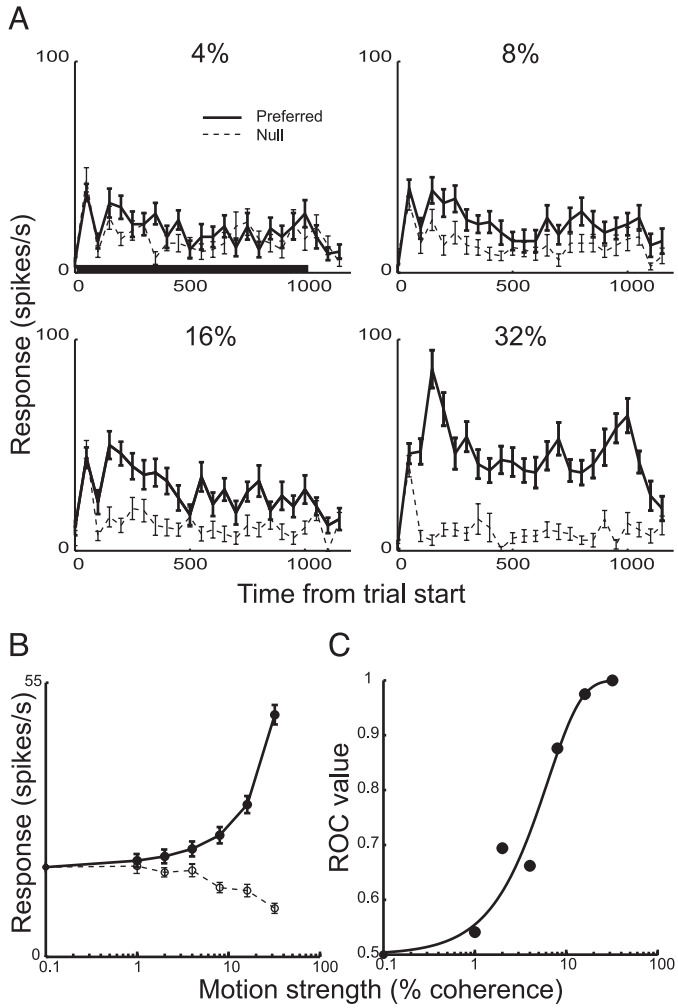

FIG. 5. *A*: responses of a single neuron to 4 levels of motion strength. Solid black line, stimulus duration. Responses were calculated in 50-ms bins; data are plotted at the beginning of bin. Error bars indicated SE over 20 trials. *B*: responses for the same neuron as a function of coherence calculated for the full 1-s duration as described in M[SCAP]ETHODS. *C*: resulting receiver operator characteristic (ROC) values; solid line, best-fit Quick function. Parameters for this cell were $\alpha_n = 6.29$ and $\beta_n = 1.17$.

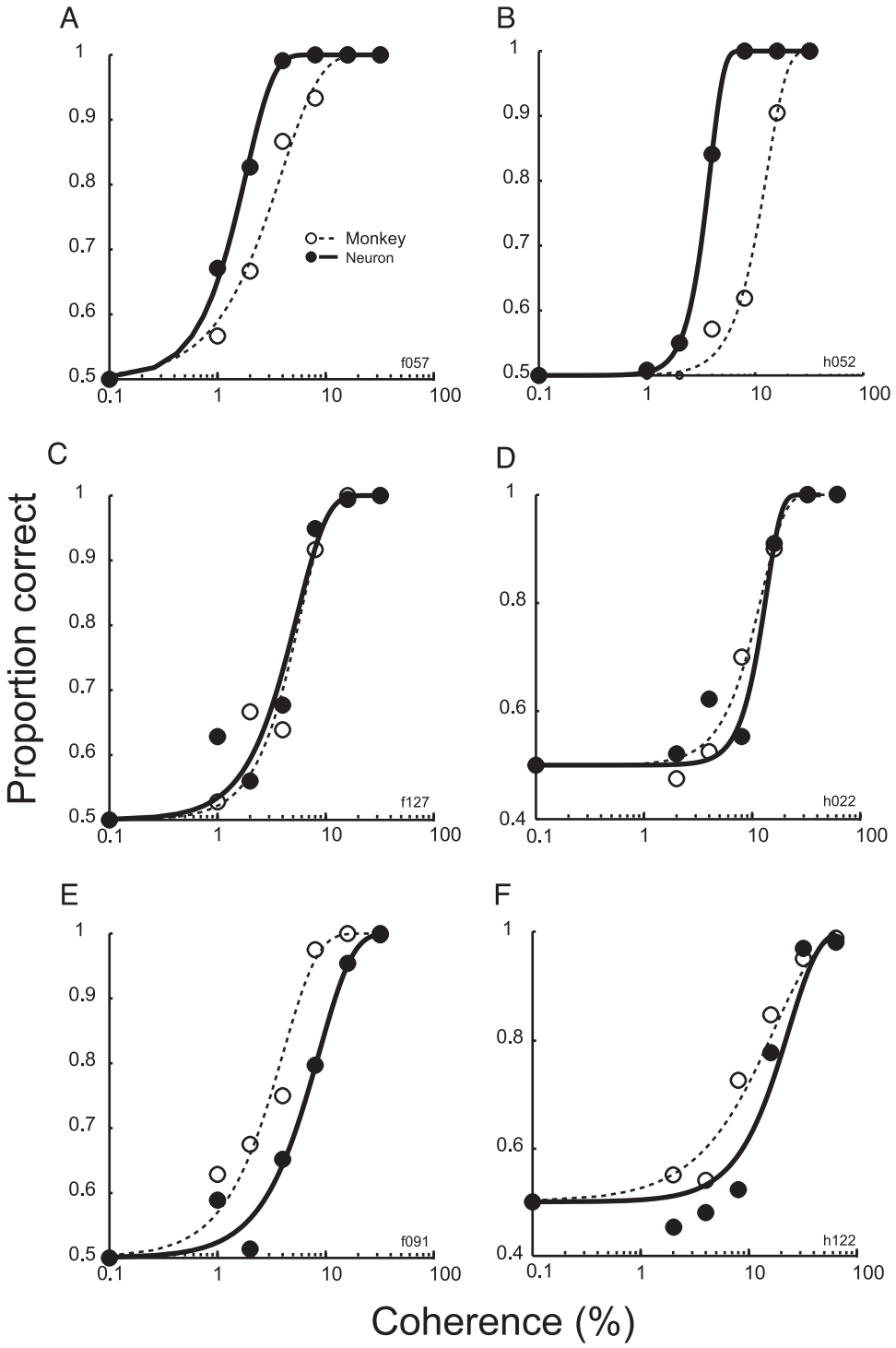

FIG. 6. Example psychometric and neurometric comparisons. Dashed lines and open circles, behavioral performance; solid lines and filled symbols, neurometric data. Data in *left column* are from monkey F; data in *right column* are from monkey H. Parameters are given 1st for the psychometric function α_p,β_p and followed by the neurometric α_n,β_n. *A*: 3.89, 1.20; 1.84, 1.69. *B*: 12.98,2.37; 3.84, 3.40. *C*: 5.86, 1.76; 5.45, 1.56. *D*: 12.32, 2.01; 13.54, 3.11. *E*: 4.051, 1.35; 8.71, 1.39. *F*: 13.09, 1.05; 23.32, 1.55.

F). Both monkeys showed a wide array of results, with some cells falling into each category of more, less, or equally sensitive relative to the simultaneously collected psychophysics.

For the majority of cases in our sample, the neurometric and psychometric functions appeared to differ from each other. To quantify these differences, we calculated the ratios between the neuronal and psychophysical thresholds. A ratio greater than unity implies that the neuron was less sensitive than the monkey. Because the two monkeys differed in their behavioral performance, we analyzed the results separately for each monkey. The resulting distributions of threshold ratios are seen in Fig. 7*A*. There was a significant difference in the threshold ratio distributions between the two monkeys (t on log-transformed ratios = 3.315, $P = 0.0013$). For monkey F, the mean threshold ratio was 2.01, indicating that neurons in MST were, on average, much less sensitive than behavioral performance. In contrast, for monkey H, neuronal and behavioral thresholds were much more similar; the mean threshold ratio being 1.11.

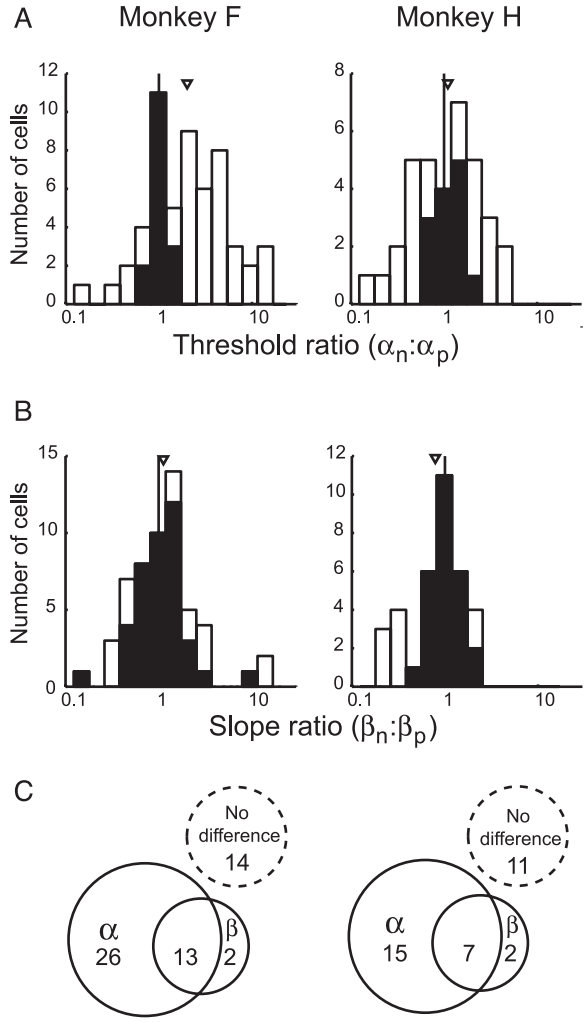

FIG. 7. Data from monkey F are in *left column*; data in *right column* are from monkey H. *A*: distribution of threshold ratios for the population. Ratios are calculated as α_n:α_p and are derived from fits with both threshold and slope allowed to vary. Values less than 1 indicate that neuronal threshold was lower (more sensitive) than behavioral threshold (see Fig. 6*A*). Open bars, cases with a significant improvement when data were fit with 2 separate functions, differing only in threshold, compared with a single function fit to both neuronal and psychometric data (nested log-likelihood test, df = 2). Solid bars, cases where the neuronal and behavioral data are not statistically distinguishable. ▽, population mean. *B*: slope ratios, calculated as β_n/β_p. ▽, population mean. *C*: distribution of cases for psychometric and neurometric comparisons. Dashed circle, experiments where both sets of data can be well described by a single function. Solid circles, experiments where significant improvement in fit was obtained by allowing either α or β to vary; note large overlap.

To address the statistical reliability of these differences between neuronal and psychophysical thresholds, we tested the hypothesis that both sets of data could be fit by a single function. We used nested log-likelihood testing to determine whether the functions differed reliably. For 25/90 cells (28%), a single function well described both sets of data for the experiment; we could not reject the null hypothesis that a single threshold and slope described both data sets (Fig. 7, filled bars).

Both monkeys showed a wide range of threshold ratios, indicating that the relationship between neuronal and perceptual sensitivity is diverse in our population of MST cells. Observed ratios for monkey F ranged between 0.14 and 13.95, while those for monkey H were between 0.16 and 4.2. The maximum possible ratio for monkey H was lower due to the higher psychophysical thresholds, described earlier. For monkey F, 22/55 (40%) cells were as sensitive as or more sensitive than the simultaneously measured psychophysical performance; for monkey H, the percentage was much higher (24/35; 69%). Thus we see that while the threshold ratios were quantitatively different for the two monkeys, there was nearly complete overlap as well. As we will show below, the only factor contributing to this difference in threshold ratios is the lower perceptual thresholds for monkey F.

Unlike the thresholds, the slopes of neurometric and psychometric functions were consistently quite similar. When we compared neurometric and psychometric slopes by measuring the ratio of the β parameters of the two functions, the mean slope ratio was 0.98 across the population. The distributions of slope ratios are shown in Fig. 7*B*. There was a tendency for the slope ratio to be lower for monkey H. However, this tendency did not produce a significant difference between monkeys ($t = 1.639$, $P > 0.05$); mean slope ratios were 1.12 and 0.86 for monkeys F and H, respectively.

For both monkeys, approximately one-quarter of all cases (15/55 for monkey F; 9/35 for monkey H) showed a significant improvement when fit with two functions differing only in their slopes. Each monkey had a substantial overlap between these cells and the group that were better fit when the threshold was free (Fig. 7*C*). For the cases that fell into the overlap category, we could evaluate which parameter better captured the data by comparing the residual errors. Because these fits had the same number of free parameters, the fit that better captured the data had a smaller residual error. For the vast majority of these cases, allowing α to vary captured the data better. Thus even for the neurometric functions that differed from the psychometric functions in both parameters, the larger difference was in the thresholds, indicating that the primary discrepancies between neurometric and psychometric functions reflect differences in sensitivity.

The difference in threshold ratios between the two monkeys could primarily be attributed to the difference in psychophysical performance. Neuronal thresholds for both monkeys varied, and the mean neuronal sensitivity did not differ between the two monkeys ($t = -1.775$; $P > 0.05$). Therefore we can conclude that the two monkeys differed far more in their performance than could be accounted for by differences in the sensitivities of their MST cells.

Although the ratios between neuronal and psychophysical threshold were diverse, there was a significant relationship between the two measures of sensitivity ($P = 0.006$; Spearman rank-order correlation). When the data from each monkey was considered individually, the relationship was only significant for one monkey, monkey H ($P = 0.0011$). The relationship between neuronal and perceptual performance was steep (Fig. 8), consistent with the fact that there was much more variance in neuronal than perceptual thresholds.

We found the presence of such a correlation puzzling, because we previously had established that no stimulus variable systematically predicts perceptual threshold. We extended this analysis to the neuronal thresholds, with similar results. Thus the relationship between neuronal and behavioral threshold could not be fully explained by the stimulus parameters we explored. For both monkeys, neuronal thresholds were statis-

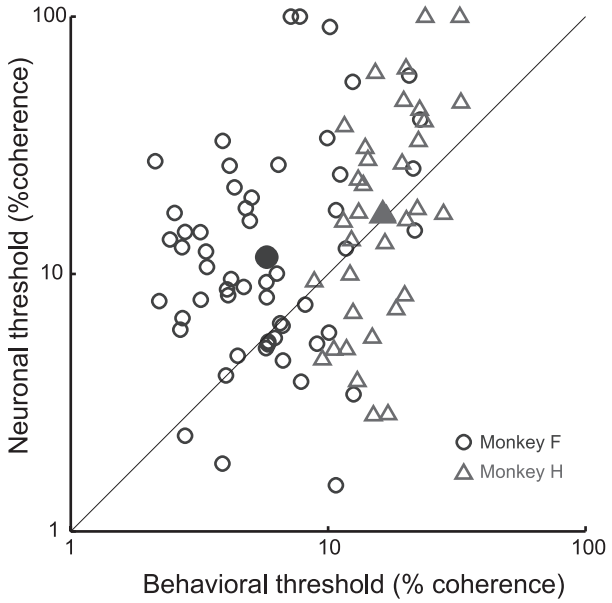

FIG. 8. Relationship between behavioral and neuronal thresholds for each monkey. Large filled symbols are geometric means.

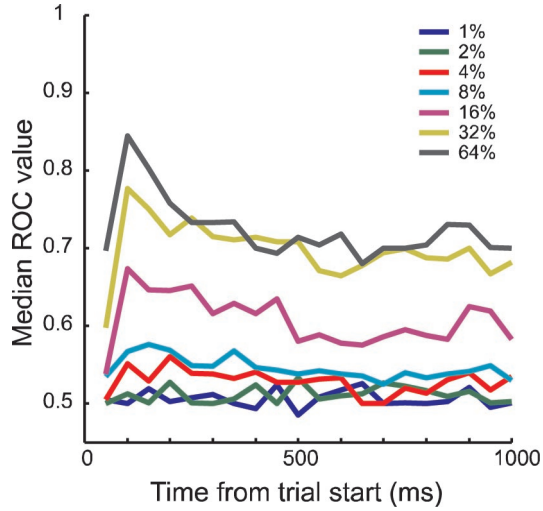

FIG. 9. Time course of selectivity. Each line represents median ROC value for the population for a single level of motion strength, calculated in 50-ms bins. Data are plotted at the beginning of bin.

tically not related to stimulus direction, speed, or eccentricity. However, neuronal thresholds from monkey H did show significant correlation with stimulus diameter ($r = 0.394$; $P = 0.0192$). In contrast, the behavioral thresholds from this monkey showed the opposite pattern; psychophysical sensitivity for monkey H was largely controlled by stimulus eccentricity and was unaffected by the size of the stimulus. Because the neuronal thresholds for the two monkeys were not affected by the stimulus parameters in the same manner as the psychophysical thresholds, the relationship between the two measures could not be explained by joint dependence on stimulus parameters. Given the absence of independent variables under our control that could jointly correlate with both neuronal and perceptual thresholds, we conclude that the most likely interpretation of this correlation is uncontrolled variability in attention or arousal.

Temporal dynamics of neuronal responses

Our primary analysis comparing neuronal and behavioral discrimination used the spike counts from the entire stimulus duration; however, this long integration window could obscure subtleties in the neuronal signal and might affect our main results. The neuronal signal of direction could either accumulate slowly or appear rapidly near the beginning of the trial. As seen in the single cell example (Fig. 5), spike rates diverged early in the trial, suggesting the latter model. We examined the dynamics of neuronal performance as a function of coherence using higher time resolution. Because neuronal thresholds did not differ between the two monkeys, this analysis was applied to the entire sample of 90 cells. For each cell, we divided the trial into 50-ms time bins and calculated the ROC value in each time window for each motion strength level.

The neuronal signals appeared quickly; for all coherence levels, the ROC value arose early (within the 1st 200 ms of the trial) and was relatively flat throughout the trial, as seen for our sample of 90 cells in Fig. 9. At the highest coherences, the ROC value initially rose more steeply but plateaued at a slightly lower level for the remainder of the stimulus duration. Not unexpectedly, the maximal value achieved for the highest coherence was <1.0; the smaller time windows reduced the number of spikes available for the calculation, and the range of different absolute sensitivities further reduced the average sensitivity. The temporal dynamics observed suggest that sensitive information was available early in the trial.

The early onset of neuronal sensitivity, coupled with its persistence throughout the trial, suggests that shorter integration times may be sufficient to achieve maximal sensitivity. To investigate this possibility, we systematically increased integration time in 50-ms intervals and calculated the threshold (α_n) for each cell as a function of integration time (Fig. 10*A*). Note that α_n sharply declined over the first 400–500 ms of the trial and then leveled out to a gradual improvement in performance as additional integration time was allowed. This flattening occurred throughout the population and was not driven solely by the less sensitive cells. To quantify this threshold asymptote as a function of time, we calculated, for each cell, the ratio between thresholds early in the integration period (400 ms) and late (the full 1-s duration). The distribution of these ratios is shown in Fig. 10*B*; the mean ratio is 1.26. This shows that, on average, the neuronal threshold only improved by

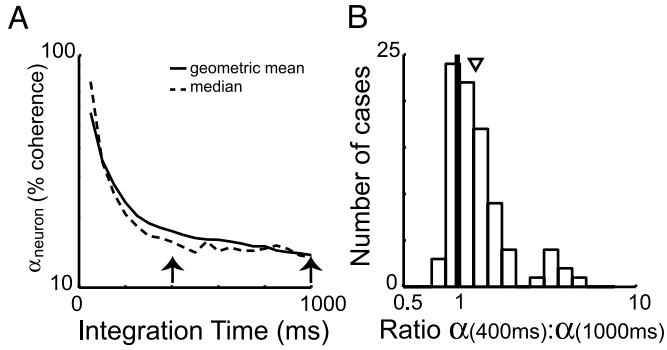

FIG. 10. Effects of integration time on neuronal threshold; integration time was incremented in 50-ms steps. *A*: population results: solid line, geometric mean of α_n for the population; dashed line, median values of the population. Arrows indicate times used for ratio calculation, as seen in *B*. *B*: distribution of ratios of α_n with 400-ms integration to α_n at the end of trial.

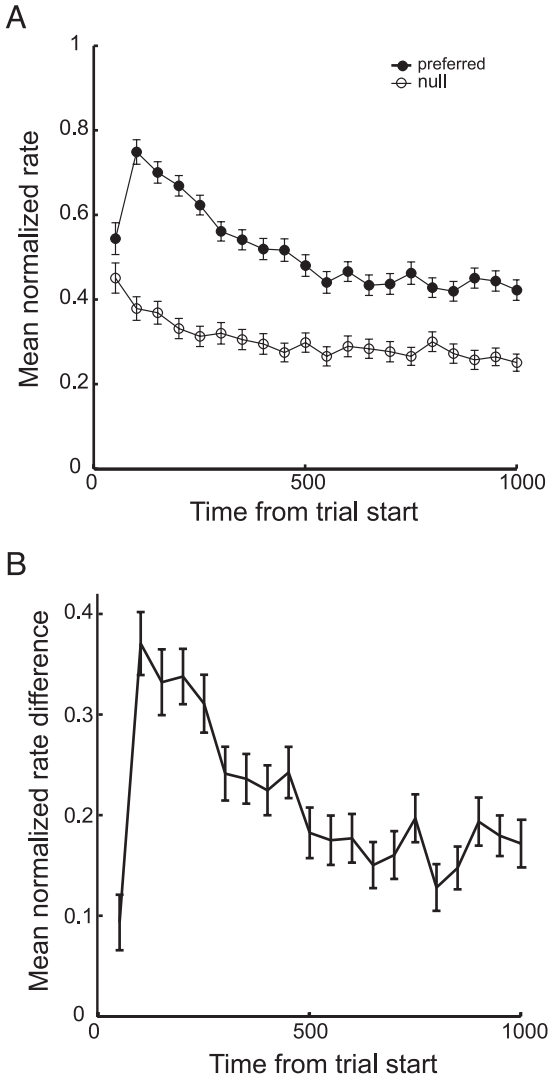

FIG. 11. *A*: average responses for preferred and null directions for 16% coherence. For each cell, both preferred and null rates were normalized to the maximal rate for preferred direction. Error bars represent SE for the population. *B*: population average of normalized rate difference between preferred and null for 16% coherence as a function of time within trial.

approximately 25% with an additional 600 ms of integration time. Some cells showed a slight increase in threshold with the longer integration times, probably due to more transient responses.

Two aspects of our data suggest that firing statistics change over the duration of a trial. First, the average ROC value for a given coherence level dropped slightly over time. Second, estimates of α_n approached a plateau around 400 ms of integration time. The drop in ROC value at later time points was due to the difference in firing rate between preferred and null responses decreasing over the course of the trial, as shown for one motion strength level (16% coherence; Fig. 11). Figure 11*A* shows the average firing rates for preferred and null directions; all rates were normalized to the maximal response for the preferred direction for the individual neuron, which could occur in any time bin. Figure 11*B* shows the decline in the difference between the null and preferred directions and revealed that the difference did plateau in the later stages of the trial.

We used a simulation to determine whether this decrease in firing rate difference was sufficient to account for the asymptotic nature of the neuronal threshold as a function of integration time. For each cell, we calculated the mean firing rates for each motion strength and direction in each 50-ms window. We then used the mean firing rate for each window to generate a Poisson distribution of spike counts for that time bin. We used these simulated trials to produce ROC values as a function of integration time and fit the results with a Quick function (*Eq. 2*) to evaluate the simulated neuronal thresholds.

There were modest, but systematic, departures of the neuronal thresholds from the simulation, indicating that the spiking statistics departed from purely Poisson predictions in two ways (Fig. 12*A*). First, the observed thresholds dropped more rapidly in the early portion of the trial than did the simulated thresholds. Second, the observed thresholds remained higher at the end of the trial than the simulation predicted. To quantify

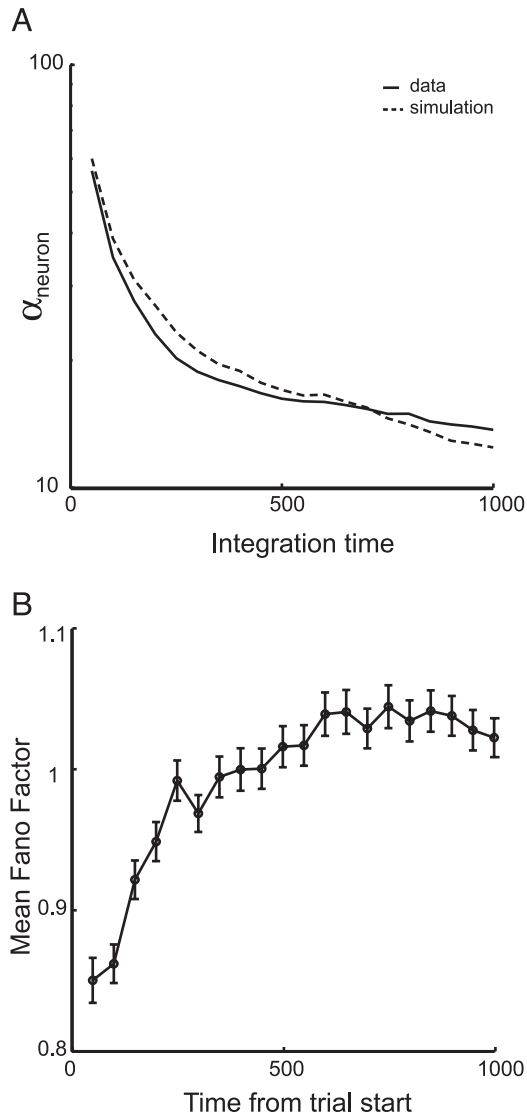

FIG. 12. *A*: observed effects of integration time on neuronal threshold compared with expected effects from a Poisson simulation with changing means. Dashed line, geometric mean of simulation predictions; solid line, geometric mean of observed effects (see also Fig. 10). *B*: variance: mean relationship changes over duration of trial. Each data point represents average Fano Factor for all conditions for all cells; error bars show SE.

this departure from Poisson statistics, we calculated the average Fano factor (variance: mean ratio) across all cells and all conditions, as a function of time within the trial. Time windows early in the trial had more reliable spiking statistics (Fano factors < 1), while late time epochs showed more variable firing (Fig. 12*B*); the average Fano factors were significantly correlated with time ($r = 0.831$; $P < 0.0001$). This was consistent with the departures of the data from the simulation and indicates that responses early in the trial may be more reliably informative about the stimulus.

Trial by trial correlation between neuronal response and behavioral choice

In many tasks for which neuronal sensitivity and perceptual sensitivity are quite similar, a signature of neuronal involvement in the task is found in the "choice probability" (Britten et al. 1996; Celebrini and Newsome 1994; Dodd et al. 2001; Parker et al. 2002). This metric captures the amount of trial-by-trial correlation between the response of a sensory neuron and the subsequent choice of the monkey. Given the correlation between neuronal and perceptual thresholds in this study, it seemed likely that a choice probability would exist in our data as well.

We explored the choice probability for our population of MST cells and were surprised to find little relationship between choice and neuronal activity on a trial-by-trial basis. We computed a single choice probability for each neuron by combining across all stimulus conditions where the monkey made at least three decisions in each direction (for details, see METHODS). Choice probability values are bounded between 0 and 1, with 0.5 representing chance (no correlation). Choice probabilities over 0.5 reveal that the neuron's response is higher for trials when monkey chooses the target representing its preferred stimulus than for null choice trials with identical stimuli.

In contrast to previous studies, we did not find a systematic correlation between firing rate and behavioral decision. For our sample of 90 neurons, the average choice probability was 0.513 (not significant, $P > 0.05$, 2-tailed *t*-test; Fig. 13). We used a permutation test to determine significance for the individual choice probabilities. The choice probability was significant for 20% (18/90) of cells; for one-half of these, the effect was backward, indicating an anti-correlation.

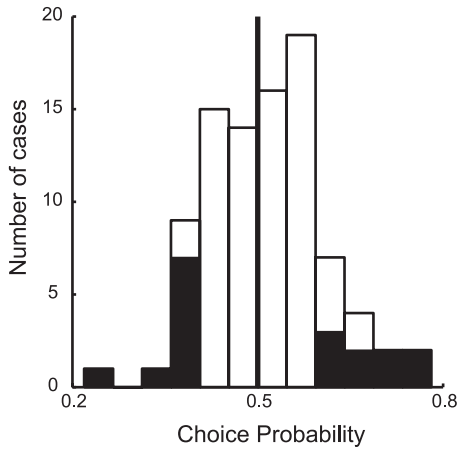

FIG. 13. Population distribution of choice probabilities. Solid bars indicate cases where the choice probability was significantly different from chance (0.5).

Despite the difference in threshold ratios between the two monkeys, there was no corresponding difference between the choice probabilities for the two monkeys. On average, monkey F had higher choice probabilities (mean = 0.52) than monkey H (mean = 0.501), but these distributions were not significantly different. This indicates that the lack of choice probability is not a reflection of differing behavioral strategies between the two monkeys.

Our observed choice probabilities were not related to neuronal response properties. There was no trend for more sensitive neurons to exhibit higher choice probabilities, as previously seen (e.g., Fig. 8, Celebrini and Newsome 1994). Similarly, there was no correlation between choice probability and threshold ratio. Intuitively, it would seem likely that cells with sensitivities most similar to the behavioral sensitivity would have a higher choice probability, but we did not observe this relationship in our data. We also examined the relationships between choice probability and dynamic range, preferred direction, and direction selectivity of the neuron under study. None of these response properties showed a significant correlation with choice probability. This suggests that the lack of significant choice probability in our data set was not due to the inclusion of insensitive or irrelevant neuronal signals.

These choice probabilities were calculated with the spike counts from the full stimulus duration, which could obscure subtleties in the time course of neuronal firing. Therefore we also investigated choice probabilities as a function of time, using the same 50-ms bins as we did for the sensitivity analysis. Previous investigations that reported significant choice probabilities in the population found that the signal accumulated early and remained constant for the duration of the trial (e.g., Britten et al. 1996). However, given that much of the observed sensitivity accumulated within the first 500 ms of the trial, it was possible that choice probabilities would be higher during the early portion of the trial, reflecting the most potent neuronal signal. Alternatively, significant choice probabilities could occur late in the trial, perhaps reflecting the upcoming decision. Neither of these possibilities was seen clearly in the data (data not shown); choice probabilities were noisy but generally flat across the trial duration. This suggests that the lack of significant choice probabilities was not a result of the time window used for analysis; choice-related activity was not consistently seen in any part of the trial.

DISCUSSION

Our experiments produced two main results. When tested with stimuli optimized in "spiral space," neurons in MST exhibited a wide range of sensitivities. Many cells had thresholds similar or superior to those measured behaviorally. While the two monkeys in this study differed substantially in their perceptual thresholds, the neurons from these animals were more similar. Another measure of neuronal involvement in a task—the choice probability—was weak or nonexistent in our data. From this pattern of results, we can assert that MST neurons are largely *sufficient* to support perceptual performance on such optic flow tasks, but in all likelihood, are not limiting for performance. It is likely that area MST works in concert with other areas to support task performance.

Complex motion analysis in MST

The neuronal sensitivities we observed support the idea that MST can provide sufficient information for perceptual analysis of optic flow. However, this does not necessarily imply that MST is *specialized* for optic flow processing, nor that the processing optic flow must occur only within MST. Instead, we believe that the wide range of relative sensitivities we obtained is likely to be a common observation at the higher levels of cortical hierarchies and may reflect the multitude of sensory processes supported by activity within MST.

While many studies have focused on the role of MST in visual motion perception, neurons in MST also respond to extraretinal signals, including eye position within the orbit (Squatrito and Maioli 1997), ocular following or pursuit eye movements (Kawano et al. 1994; Newsome et al. 1988), and vestibular input (Bremmer et al. 1999; Thier and Erickson 1992). Additionally, many neurons show selective responses to combinations of retinal motion image and extraretinal signals (Bradley et al. 1996; Duffy 1998; Upadhyay et al. 2000). Individual neurons in MST may be quite sensitive for one type of signal while being responsive but insensitive to another. This would result in a wide range of sensitivities when only a single stimulus type is explored and is consistent with our observations.

The diversity of sensory signals within MST need not imply that the representation of optic flow is "sparse," with only a small fraction of neurons actively contributing at any one time. Instead, large numbers of neurons are responsive to optic flow, with widely varying sensitivities relative to the monkey. Under these circumstances, two different pooling and decision rules are possible if the monkey is relying on the signals from MST for its perceptual judgment. First, the monkey could be using only a portion of the active neurons—those that have sensitivities close to his own. In both of our monkeys, these well-matched neurons are not the most sensitive ones, which exceed behavioral capabilities. Thus this rule would conform poorly to the "lower envelope principle" (Mountcastle et al. 1972). Alternately, the monkey could pool broadly over the population and use signal averaging to achieve higher sensitivity. The latter model is broadly consistent with our observations.

Missing choice probability

In several related experiments in the motion pathway, significant choice probabilities have been interpreted as a signature of neuronal involvement in the perceptual task. One study in particular is quite comparable to ours. Celebrini and Newsome (1994) measured both sensitivity and choice probability for MST neurons in the context of a linear direction-discrimination task. Their analysis of neuronal sensitivity revealed a pattern of results not very different from ours. Neurons were slightly more sensitive in that context, relative to the monkey, but again showed a range of sensitivities. However, choice probabilities were much larger in their study, suggesting an association between area MST and linear motion discriminations.

This difference in choice probability for two related tasks is puzzling. There are two main differences between the two tasks. The most conspicuous one lies in the stimuli: complex versus translational motion. The other difference is more subtle—our monkeys were given "matching" saccade targets at the end of the trial. These targets contained motion in the neuron's preferred and null direction. We do not believe that this latter task difference explains the lack of significant choice probabilities in our study. Significant choice probabilities have been seen during the sample period of a delayed match-to-sample task in area MT (T. Pasternak, personal communication), indicating that matching tasks do not eliminate the trial-by-trial correlation between neuronal activity and behavioral choice. Additionally, after initial inspection of the targets at the beginning of the block, the monkeys could use the position of the target for their response; target locations were constant throughout a block of trials. It seems probable that the monkeys switched to such a position strategy early in each block, since their response latencies were very short. Therefore it seems unlikely that the monkeys were performing a true matching task. Given this, we conclude that the difference in choice probabilities reflects a qualitatively different involvement in tasks requiring the analysis of complex motion.

The weak or nonexistent choice probability in our data also appears to contradict the results of microstimulation in MST during a heading discrimination task (Britten and Van Wezel 2002). Microstimulation influenced perceptual judgments of simulated heading, and those effects have been interpreted to support MST's involvement in complex motion perception. However, a number of significant effects in the microstimulation were backwards from the expected direction, suggesting that the relationship between MST activity and perception was not straightforward. Second, the horizontal headings used in those experiments contained substantial translational flow. As demonstrated by Celebrini and Newsome (1995), microstimulation in MST also affected linear discriminations. The microstimulation effects observed in the heading task may be partially due to the strong translational components in the stimuli. Taken together, these results suggest that the relationship between neuronal activity in MST and complex motion perception may be weaker than the relationship for linear motion analysis.

Interanimal differences

A curious feature of our data was that, while neuronal thresholds were on average similar for the two monkeys, behavioral thresholds were not. Monkey H had higher behavioral thresholds, resulting in lower threshold ratios. The differences between monkeys may be due to differing perceptual abilities or behavioral control issues. In three cases, monkey H had unusually high thresholds; these were sessions when the neuron's response properties dictated stimulus parameters that were less commonly encountered during training. For the remaining cases, monkey H's performance was consistent with thresholds obtained during the final stages of training, which were asymptotic against time. This indicates that the observed thresholds were an accurate reflection of perceptual ability. We also confirmed that monkey H was not strictly using local cues by testing with a foveally centered stimulus that should have encouraged such a strategy. Further support was provided by the slopes of the psychometric functions, which will be lower for monkeys inadequately motivated or performing poorly. Slopes were similar between the two monkeys and fell into an acceptable range. Therefore the observed differences between

the two monkeys cannot be attributed to differing behavioral control, and presumably, they reflect differing perceptual abilities.

Although the perceptual thresholds differed between the two animals, the neuronal thresholds did not. This contrasts with previous observations for a linear direction discrimination task in area MT (Britten et al. 1992), where both neuronal and psychophysical thresholds varied between animals in a correlated manner—animals with more sensitive behavioral thresholds also had more sensitive neurons. The difference in perceptual thresholds for our task, unaccounted for by neuronal threshold differences, strongly suggests that other areas contribute to performance and might even limit it. The additional influences on performance may lie in downstream decision mechanisms or else in the contributions of other sensory representations of optic flow information. It could be argued that the decoupling between neuronal and perceptual thresholds we observe would be consistent with MST being completely uninvolved in this task. While this is possible, it would require that perception was not using a source of sufficient signals for performance, and we find this idea less than parsimonious.

Optic flow signals in other cortical areas

Although MST clearly contains suitable neuronal signals for optic flow processing, our results suggest that optic flow perception is likely to be based on activity in multiple cortical areas, including the ventral parietal area (VIP) and parietal area 7a. Both of these areas contain neurons with similar selectivities for spiral space motion as those in MST (Schaafsma and Duysens 1996; Siegel and Read 1997), and are also good candidates for the neuronal substrate of optic flow perception. Additionally, the anterior portion of the superior temporal polysensory area (STPa) contains neurons that respond selectively to optic flow components, although they appear to be more restricted to the cardinal axes of radial and rotary motion (Anderson and Siegel 1999). Perception of complex motions patterns may depend on activity in all four areas, either hierarchically or in parallel. MST projects to VIP, 7a, and STPa (Andersen et al. 1990; Baizer et al. 1991; Boussaoud et al. 1990), suggesting sequential processing. Intuitively, this would suggest that sensitivities in one of these other areas might be greater and that neurons in these areas might exhibit higher choice probabilities than we observed in MST. Alternatively, if signals from multiple cortical areas are pooled for the task, choice probabilities would be reduced due to lesser interneuronal correlation across the areas (Shadlen et al. 1996) Therefore the most sensible conclusion to draw from our results is that MST contributes to complex motion perception, but it is likely to do so in concert with other cortical areas.

ACKNOWLEDGMENTS

We thank R. E. Tarbet, J. L. Moore, and M. R. Nilsson for technical assistance and monkey training. A. L. Jones wrote the stimulus presentation software. We thank A. M. Churchland, K. A. McAllister, G. H. Recanzone, and W. M. Usrey for valuable comments on earlier versions of the manuscript.

GRANTS

This work was supported by National Institutes of Health Grants EY-10562 and EY-12576 to K. H. Britten and MH-11700 to H. W. Heuer.

REFERENCES

Anderson KC and Siegel RM. Optic flow selectivity in the anterior superior temporal polysensory area, STPa, of the behaving monkey. *J Neurosci* 19: 2681–2692, 1999.

Andersen R, Snowden R, Treue S, and Graziano M. Hierarchical processing of motion in the visual cortex of monkey. In: *Cold Spring Harbor Symposia on Quantitative Biology, Vol. LV, The Brain.* Plain View, NY: Cold Spring Harbor Laboratory Press, 1990, p. 741–748.

Baizer JS, Ungerleider LG, and Desimone R. Organization of visual inputs to inferior temporal and posterior parietal cortex in macaques. *J Neurosci* 11: 168–190, 1991.

Boussaoud D, Ungerleider LG, and Desimone R. Pathways for motion analysis: cortical connections of the medial superior temporal and fundus of the superior temporal visual areas in the macaque. *J Comp Neurol* 296: 462–495, 1990.

Bradley A, Skottun BC, Ohzawa I, Sclar G, and Freeman RD. Visual orientation and spatial frequency discrimination: a comparison of single cells and behavior. *J Neurophysiol* 57: 755–772, 1987.

Bradley DC, Maxwell M, Andersen RA, Banks MS, and Shenoy KV. Mechanisms of heading perception in primate visual cortex. *Science* 273: 1544–1547, 1996.

Bremmer F, Kubischik M, Pekel M, Lappe M, and Hoffmann KP. Linear vestibular self-motion signals in monkey medial superior temporal area. *Ann NY Acad Sci* 871: 272–281, 1999.

Britten KH, Newsome WT, Shadlen MN, Celebrini S, and Movshon JA. A relationship between behavioral choice and the visual responses of neurons in macaque MT. *Vis Neurosci* 13: 87–100, 1996.

Britten KH, Shadlen MN, Newsome WT, and Movshon JA. The analysis of visual motion: a comparison of neuronal and psychophysical performance. *J Neurosci* 12: 4745–4765, 1992.

Britten KH and Van Wezel RJA. Electrical microstimulation of cortical area MST biases heading perception in monkeys. *Nature Neurosci* 1: 1–5, 1998.

Britten KH and Van Wezel RJA. Area MST and heading perception in Macaque monkeys. *Cereb Cortex* 12: 692–701, 2002.

Celebrini S and Newsome WT. Neuronal and psychophysical sensitivity to motion signals in extrastriate area MST of the macaque monkey. *J Neurosci* 14: 4109–4124, 1994.

Celebrini S and Newsome WT. Microstimulation of extrastriate area MST influences performance on a direction discrimination task. *J Neurophysiol* 73: 437–448, 1995.

Chandler JP. STEPIT: University of Indiana Quantum Chemistry Program Exchange, 1965.

Crist CF, Yamasaki DSG, Komatsu H, and Wurtz RH. A grid system and a microsyringe for single cell recording. *J Neurosci Methods* 26: 117–122, 1988.

DeAngelis GC and Uka T. Coding of horizontal disparity and velocity by MT neurons in the alert macaque. *J Neurophysiol* 89: 1094–1111, 2003.

Desimone R and Ungerleider LG. Multiple visual areas in the caudal superior temporal sulcus of the macaque. *J Comp Neurol* 248: 164–189, 1986.

Dodd JV, Krug K, Cumming BG, and Parker AJ. Perceptually bistable 3-D figures evoke high choice probabilities in cortical area MT. *J Neurosci* 21: 4809–4821, 2001.

Duffy CJ. MST neurons respond to optic flow and translational movement. *J Neurophysiol* 80: 1816–1827, 1998.

Duffy CJ and Wurtz RH. Sensitivity of MST neurons to optic flow stimuli. I. A continuum of response selectivity of large-field stimuli. *J Neurophysiol* 65: 1329–1345, 1991a.

Duffy CJ and Wurtz RH. Sensitivity of MST neurons to optic flow stimuli. II. Mechanisms of response revealed by small-field stimuli. *J Neurophysiol* 65: 1346–1359, 1991b.

Duffy CJ and Wurtz RH. Response of monkey MST neurons to optic flow stimuli with shifted centers of motion. *J Neurosci* 15: 5192–5208, 1995.

Froehler MT and Duffy CJ. Cortical neurons encoding path and place: where you go is where you are. *Science* 295: 2462–2465, 2002.

Geesaman BJ and Andersen RA. The analysis of complex motion patterns by form/cue invariant MSTd neurons. *J Neurosci* 16: 4716–4732, 1996.

Gibson JJ. *Perception of the Visual World.* Boston, MA: Houghton-Mifflin, 1950.

Gold JI and Shadlen MN. Banburismus and the brain: decoding the relationship between sensory stimuli, decisions, and reward. *Neuron* 36: 299–308, 2002.

Graziano MSA, Andersen RA, and Snowden RJ. Tuning of MST neurons to spiral motions. *J Neurosci* 14: 54–67, 1994.

Green DM and Swets JA. *Signal Detection Theory and Psychophysics.* New York: John Wiley, 1966.

Hays AV, Richmond BJ, and Optican LM. A UNIX-based multiple process system for real-time data acquisition and control. *WESCON Conf Proc* 2: 1–10, 1982.

Heuer HW and Britten KH. Comparison of perceptual and neural sensitivity to optic flow patterns in macaque area MST. *Soc Neurosci Abstr* 25, 1999.

Heuer HW and Britten KH. The relationship between behavioral choice and neuronal activity in extrastriate area MST during a complex motion discrimination task. *Soc Neurosci Abstr* 251.5, 2000.

Hoel P, Port S, and Stone C. *Introduction to Statistical Theory*. Boston, MA: Houghton Mifflin Company, 1971.

Judge SJ, Richmond BJ, and Chu FC. Implantation of magnetic search coils for measurement of eye position: an improved method. *Vision Res* 20: 535–538, 1980.

Kawano K, Shidara M, Watanabe Y, and Yamane S. Neural activity in cortical area MST of alert monkey during ocular following responses. *J Neurophysiol* 71: 2305–2324, 1994.

Mardia KV and Jupp PE. *Directional Statistics.* New York: Chichester, 2000.

Mountcastle V, LaMotte R, and Carli G. Detection thresholds for vibratory stimuli in humans and monkeys; comparison with threshold events in mechanoreceptive first order afferent nerve fibrers innervating monkey hands. *J Neurophysiol* 35: 122, 1972.

Newsome WT, Wurtz RH, and Komatsu H. Relation of cortical areas MT and MST to pursuit eye movements. II. Differentiation of retinal from extraretinal inputs. *J Neurophysiol* 60: 604–620, 1988.

Orban GA. Visual processing in macaque area MT/V5 and its satellites (MSTd and MSTv). In: *Cerebral Cortex*, edited by Rockland KS, Kaas JH, and Peters A. New York: Plenum, 1997, p. 359–434.

Page WK and Duffy CJ. MST neuronal responses to heading direction during pursuit eye movements. *J Neurophysiol* 81: 596–610, 1999.

Paolini M, Distler C, Bremmer F, Lappe M, and Hoffmann KP. Responses to continuously changing optic flow in area MST. *J Neurophysiol* 84: 730–743, 2000.

Parker AJ, Krug K, and Cumming BG. Neuronal activity and its links with the perception of multi-stable figures. *Philos Trans R Soc Lond B Biol Sci* 357: 1053–1062, 2002.

Quick RF. A vector magnitude model of contrast detection. *Kybernetik* 16: 65–67, 1974.

Saito H, Yukie M, Tanaka K, Hikosaka K, Fukada Y, and Iwai E. Integration of direction signals of image motion in the superior temporal sulcus of the macaque monkey. *J Neurosci* 6: 145–157, 1986.

Schaafsma SJ and Duysens J. Neurons in the ventral intraparietal area of awake macaque monkey closely resemble neurons in the dorsal part of the medial superior temporal area in their responses to optic flow patterns. *J Neurophysiol* 76: 4056–4068, 1996.

Shadlen MN, Britten KH, Newsome WT, and Movshon JA. A computational analysis of the relationship between neuronal and behavioral responses to visual motion. *J Neurosci* 16: 1486–1510, 1996.

Siegel RM and Read HL. Analysis of optic flow in the monkey parietal area 7a. *Cereb Cortex* 7: 327–346, 1997.

Squatrito S and Maioli MG. Gaze field properties of eye position neurones in areas MST and 7a of the macaque monkey. *Vis Neurosci* 13: 385–398, 1996.

Squatrito S and Maioli MG. Encoding of smooth pursuit direction and eye position by neurons of area MSTd of macaque monkey. *J Neurosci* 17: 3847–3860, 1997.

Tanaka K, Fukada Y, and Saito H. Underlying mechanisms of the response specificity of expansion/contraction and rotation cells in the dorsal part of the medial superior temporal area of the Macaque monkey. *J Neurophysiol* 62: 642–656, 1989.

Tanaka K, Hikosaka H, Saito H, Yukie Y, Fukada Y, and Iwai E. Analysis of local and wide-field movements in the superior temporal visual areas of the macaque monkey. *J Neurosci* 6: 134–144, 1986.

Tanaka K and Saito H. Analysis of motion of the visual field by direction, expansion/contraction and rotation cells clustered in the dorsal part of the medial superior temporal area of the Macaque monkey. *J Neurophysiol* 62: 626–641, 1989.

Thier P and Erickson RG. Vestibular input to visual-tracking neurons in area MST of awake rhesus monkeys. *Ann NY Acad Sci* 656: 960–963, 1992.

Upadhyay UD, Page WK, and Duffy CJ. MST responses to pursuit across optic flow with motion parallax. *J Neurophysiol* 84: 818–826, 2000.

Van Essen DC, Maunsell JHR, and Bixby JL. The middle temporal visual area in the macaque: myeloarchitecture, connections, functional properties and topographic representation. *J Comp Neurol* 199: 293–326, 1981.